4D computed tomography assessment of ruptured triple-lumen type B aortic dissection: a case report

Ying Li [1]*[†]**, Jia Li** [2][†]**, Jia Chen** [3]**, and Pei qun Zhao** [4]

[1]Department of Digital Medicine, College Biomedical Engineering and Medical Imaging, Army Medical University (Third Military Medical University), Chongqing 400038, China; [2]Department of Emergency, The Second Affiliated Hospital, Army Medical University (Third Military Medical University), Chongqing 400030, China; [3]Department of Radiology, The Second Affiliated Hospital, Army Medical University (Third Military Medical University), Chongqing 400030, China; and [4]Department of Cardiac Surgery, The Second Affiliated Hospital, Army Medical University (Third Military Medical University), Chongqing 400030, China

Background	Few studies have investigated the effect of the intimal morphology of type B aortic dissection (TBAD) on the blood flow after rupture. We report a case of a 30-year-old male with complicated TBAD, who underwent assessment with 4D computed tomography (4D-CT).
Case summary	Patient presented with chest tightness for 14 days, a heart rate of 67 b.p.m., regular rhythm, and 2 years of hypertension. Precisely 14 days prior, he had been diagnosed with aortic dissection by ultrasound at another hospital. 4D-CT showed thoracoabdominal aortic dissection (Stanford type B), left haemothorax, multiple dissection tears, an initial tear located at the large curvature side of the aortic arch, a proximal tear entrance >15 mm, and a descending aorta exit >5 mm. 4D-CT analysis and visualization of the intimal flap showed a parallel three-lumen spatial morphology of true–false–true, and the lumen showed partial thrombosis in the false lumen. Further quantitative analysis of the area of the initial and re-entry tear during the cardiac cycle revealed that the ratio of the initial tear to re-entry tear was consistent with the expansion ratio of the false lumen to the true lumen of the re-entry tear. The patient improved and was discharged 1 week after undergoing thoracic endovascular aortic repair (TEVAR) for descending aortic dissection.
Discussion	The complex triple-lumen TBAD, characterized by multiple tears and blood flow channels, poses challenges for TEVAR. 4D-CT facilitates the visualization of intimal flap spatial distribution and enables a thorough assessment of interlayer dilation risk within a realistic and complex haemodynamic context, thereby refining the risk stratification for the progression of complicated aortic dissection and its associated complex complications.
Keywords	4D-CT • Ruptured type B aortic dissection • Triple lumen • Haemothorax • Intimal flap • Case report
ESC curriculum	2.4 Cardiac computed tomography • 9.1 Aortic disease

---

Learning points

- A true–false–true three-lumen configuration is rare, and this intricate structural alteration complicates blood flow distribution within the aorta.
- By utilizing 3D re-construction, the spatial distribution of the intimal flap within the aortic lumen and the distribution of blood flow obstructions can be observed.
- 4D-CT imagery enables the observation of the influence of blood flow on the oscillatory motion of a torn intimal flap at the intimal tear site.

Introduction

The annual incidence of aortic dissection is ~3–16 per 100 000 people,[1] and the mortality rate in untreated patients can be as high as 1%–2%/h. The mortality rate of acute type B aortic dissection (TBAD) increases by 20% daily due to complex situations such as poor perfusion or rupture.[2] If the initial dissection tear in a TBAD is located in the large curvature of the aortic arch, the risks of a large primary tear, aortic periaortic haematoma, and haemothorax are high.[3] Acute-on-chronic triple-lumen TBAD accounts for only 2.9% of type B dissection cases and, although relatively rare, is associated with a higher overall mortality rate.[4] Few patients with aortic rupture or haemothorax survive, and our understanding of their blood flow status remains limited. This study reports a case of triple-lumen aortic dissection after TBAD rupture and analyses the spatial morphology and geometric characteristics of the aortic dissection intimal flap using 4D computed tomography (4D-CT).

Summary figure

Date	Event description
18 October 2023	The patient presented with chest tightness and was diagnosed with 'aortic dissection' by ultrasound at a local hospital. Treatment was recommended, but the patient refused.
1 November 2023	The patient was admitted to the emergency department of the Second Affiliated Hospital of Army Medical University. Sixty-four-slice computed tomography angiography confirmed type B aortic dissection, while 4D-CT revealed a ruptured triple-lumen acute-on-chronic variant. The patient received endovascular stent grafting for descending aortic dissection.
3 November 2023	Ultrasound-guided thoracentesis was performed.
7 November 2023	The patient was discharged from the hospital.
6 December 2023	The patient attended a follow-up appointment at the Cardiothoracic Surgery Clinic. Partial thrombus formation was observed in the false lumen.

Case presentation

The patient was a 30-year-old male with body mass index of 30.59 kg/m^2 who was admitted to the hospital due to chest tightness for 14 days, accompanied by numbness in his hands and feet. He had a history of smoking and 2 years of hypertension, and was diagnosed with aortic dissection using ultrasonography at another hospital. Seeking more advanced surgical intervention, the patient chose to transfer from primary care to a higher-level medical facility.

Upon admission, his blood pressure and heart rate were 152/84 mmHg and 67 b.p.m., respectively. Electrocardiography revealed no apparent abnormalities. Laboratory findings were as follows: creatinine, 111.3 μmol/L; D-dimer, 1.23 mg/L; white blood cell count, 9.71×10^9/L; C-reactive protein, 52.6 mg/L; and brain natriuretic peptide, 78.9 pg/mL. Arterial blood gas analysis revealed a pH of 7.45, PCO_2 of 34 mmHg, PO_2 of 80 mmHg, and lactate of 0.6 mmol/L. For this cardiac imaging study, we used an imaging protocol to achieve high-resolution scanning. Key parameters included a temporal resolution of 280 ms and a slice thickness of 0.6 mm across 128 detector rows. The scan was conducted at a tube voltage of 100 kV, synchronized with the entire cardiac cycle using retrospective electrocardiographic gating. The gating scan covers the area from the lung apex to 3 cm below the pubic symphysis. Optimal vascular opacification was achieved by infusing the contrast agent, iodixanol, at a rate of 4.2 mL/s with a concentration of 350 mg per 100 mL. Post-processing involved reconstructing the raw data at 10% intervals of the cardiac cycle to capture dynamic cardiac changes. 4D-CT revealed Stanford TBAD (*Figure 1*), partial atelectasis

of the left lung, inflammation in the lower lobes of both lungs, and haemothorax in the left thoracic cavity (*Figure 1D*). 4D-CT analysis and visualization of the intimal flap showed a parallel triple-lumen spatial morphology of true–false–true (*Figure 2*), multiple dissection tears, and an initial tear located at the large curvature side of the aortic arch. The diameters were as follows: proximal tearing entrance in the aorta, >41 mm; exit in the descending aorta, >44 mm; false lumen, >25 mm; primary tearing entrance, >15 mm; and re-entrance in the descending aorta, >5 mm. The distance between the entrance and re-entrance was >110.99 mm (*Figure 2A*). The haemorrhage site in the thoracic cavity is identified as the descending aorta (*Figure 3A*). The blood supply to the abdominal organs is maintained through the true lumen of the superior mesenteric artery and partial false lumen of the coeliac trunk, and partial thrombosis occurred in the false lumen (*Figure 3B*).

Under general anaesthesia, the patient underwent endovascular exclusion to treat the descending aortic dissection, using a 34 × 200 mm covered stent from Cook Medical's endovascular stent graft portfolio. Contrast agent was administered stepwise through the vascular sheath to locate the true lumen up to the ascending aorta. Under fluoroscopic guidance, a thoracic aortic covered stent system was positioned along a stiff guidewire, with the stent placed 2 cm from the proximal tear on the normal vessel wall (*Figure 5*). Two days after surgery, the patient underwent an ultrasound-guided left thoracentesis, significantly alleviating the patient's chest tightness symptoms. The patient's vital signs remained stable, and the surgical wound healed excellently. The patient was deemed fit for discharge 1 week post-operatively. A follow-up chest radiograph conducted 2 months post-operatively revealed a reduction in the left haemothorax observed prior to surgery. The patient remains asymptomatic 5 months post-surgery, with ongoing regular follow-ups.

Discussion

Here, we present a case of a patient with a complicated TBAD, where 4D-CT facilitated the analysis of the triple-lumen spatial structure and associated vascular changes. Haemothorax is a serious feature of complexed TBAD, posing a significant risk of acute blood loss and precipitating life-threatening conditions. Multiple studies demonstrate that thoracic endovascular aortic repair (TEVAR) enhances survival, reduces aortic complications, and improves long-term prognosis in complicated TBAD. The European Society of Cardiology guidelines[5] recommend that TEVAR be used for acute or subacute complicated TBAD. But triple-lumen dissection is relatively rare. The morphology of the torn intima makes the blood flow environment in the multi-lumen aorta very complex,[6] with a high risk of complications and rupture. In most
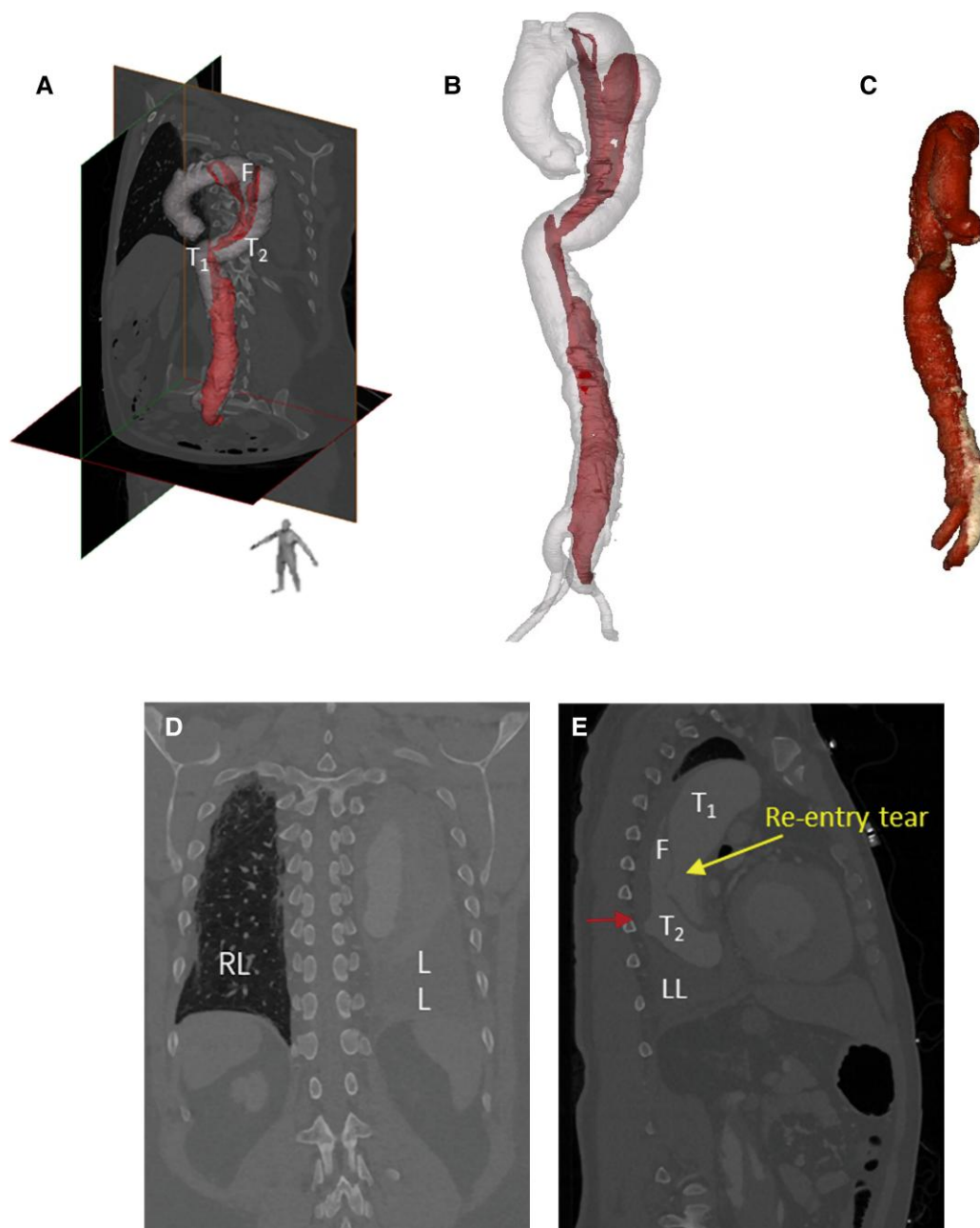
Figure 1 Analysis of 10 phases of 4D computed tomography angiography images using Mimics software showed the spatial morphology of type B aortic dissection. (*A, B*) 3D geometry of the aortic dissection model constructed from computed tomography angiography images. (*C*) Volume-rendered 3D models based on computed tomography. (*D*) Haemothorax in the left lung. (*E*) Location of blood infiltration (red arrow).

triple-lumen cases, two false lumens wrap around the true lumen. A true–false–true trilumen aorta (*Figure 3*) has not yet been reported. This anatomical configuration presents challenging access and potential difficulties in guidewire and catheter navigation during the implantation procedure.

Triple-lumen dissection frequently signifies multiple tears and blood flow pathways, and the effect of residual tears on haemodynamics following stent coverage of the proximal tears remains uncertain. 4D-CT, also known as electrocardiogram-gated CT, significantly reduces motion artefacts, enhances edge delineation, and minimizes measurement variability.[7] This technique facilitates observation of aortic wall motion, haemodynamic alterations, and dynamic dissection expansion. In this case, high pressure in the false lumen caused the collapse of the true lumen T_1, and blood flowed from the false lumen into the true lumen T_2 through the re-entry tear, with the dissection spreading to the iliac artery (*Figure 2B*). The thrombus formed part of the false lumen of the coeliac trunk (*Figure 2B*). Assuming stent deployment in the T_1 true lumen compresses the false lumen, blood flows through the T_2 true
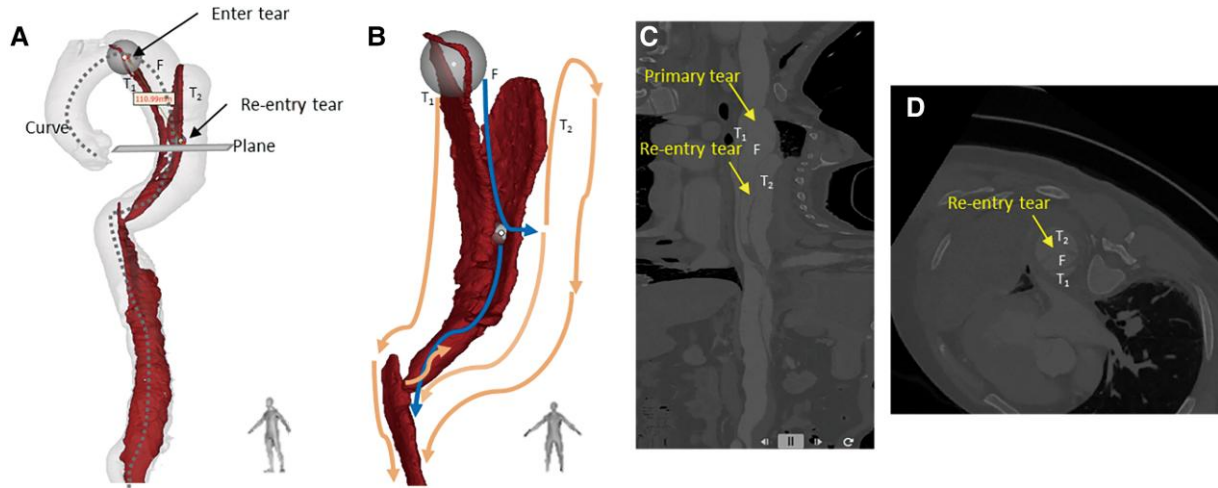
Figure 2 3D segmentation model of the aortic flap tear and 4D computed tomography dynamic images at 10 phases of the cardiac cycle. (A) Aorta 3D model with intimal flap showed that the false lumen was between two true lumens like a 'sandwich'. The diameters were as follows: proximal tearing entrance in the aorta, >41 mm; exit in the descending aorta, >41 mm; false lumen, >25 mm; primary tearing entrance, >15 mm; and re-entrance in the descending aorta, >5 mm. The distance between the entrance and re-entrance was >110.99 mm. (B) Blood flows from the true lumen (T_1) into the false lumen through the primary tear and then returns to the true lumen (T_2) through the re-entry tear. The blue and orange lines represent the potential blood flow paths in the false and true lumens, respectively. After blood enters T_2 through the re-entry tear, some of it travels up to the top of the aortic arch, while the rest follows the flow in the true lumen to the descending aorta. These streams converge at the diaphragm, where, due to an obstruction caused by partial thrombosis formation, a portion of the blood flows back into the false lumen through the tear opening, while the remainder continues towards the abdominal aorta. (C) Curve plane re-construction of (A) with straightened cine angiography of the vessel. (D) Plane of (A) perpendicular to the re-entry tear, with very little residual endothelial flap at the entrance, as seen in cine imaging, was smaller than that of the re-entry tear.
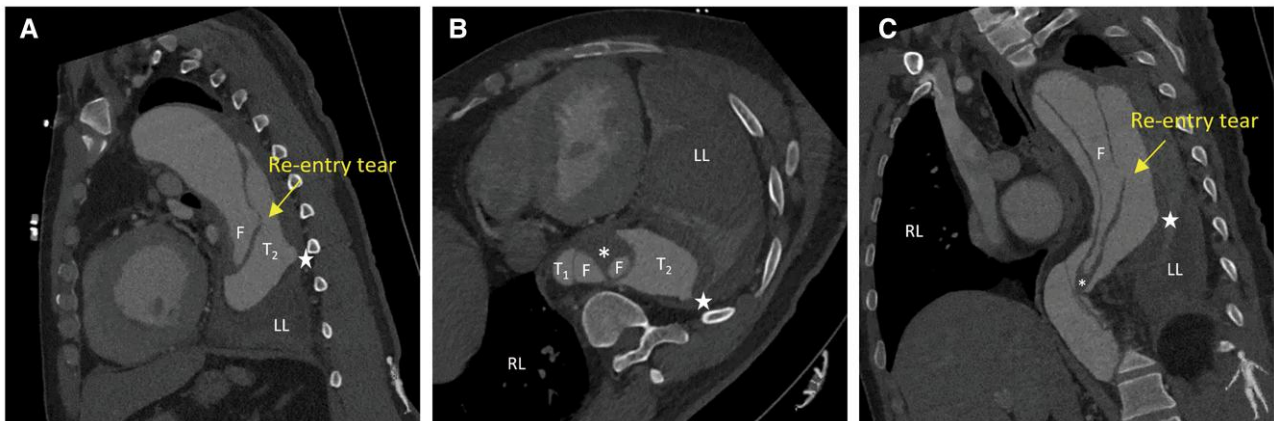

Figure 3 4D computed tomography scans showing the movie images of the true and false lumens and intimal flaps moving with blood flow from different perspectives. (A) Coronal section. (B) Axial section. (C) Sagittal section. Four highlighted areas appear in aortic lumen (T_1 and T_2 in the true lumen and two F in the false lumen), not signifying four separate cavities but depicting complex patterns due to partial thrombosis in the false cavity alongside active blood flow. The pentagram represents the site of blood leakage from the aortic rupture. The rupture site of the aneurysm was visible on the dorsal side of the descending aorta, and the complex blood flow inside the lumen and haemorrhage around the blood vessel wall is visible. During cardiac cyclic motion, the flap site vibrated within the true and false lumens, and partial thrombosis occurred in the false lumen (asterisk in B). RL, right lung; LL, left lung.

lumen (*Figure 2C*) to prevent excessive pressure and potential rupture, as verified by intraoperative digital subtraction angiography (*Figure 5A*). Partial thrombosis within the abdominal aorta may contribute to dissection stabilization. Previous studies have shown that tear size is associated with blood flow velocity.[8,9] In this case, the diameter ratio of the initial entry tear to the re-entry tear was 3:1. During the cardiac cycle, the changes in area of the false lumen are greater than those in the area of the true lumen (*Figure 4A and C*).
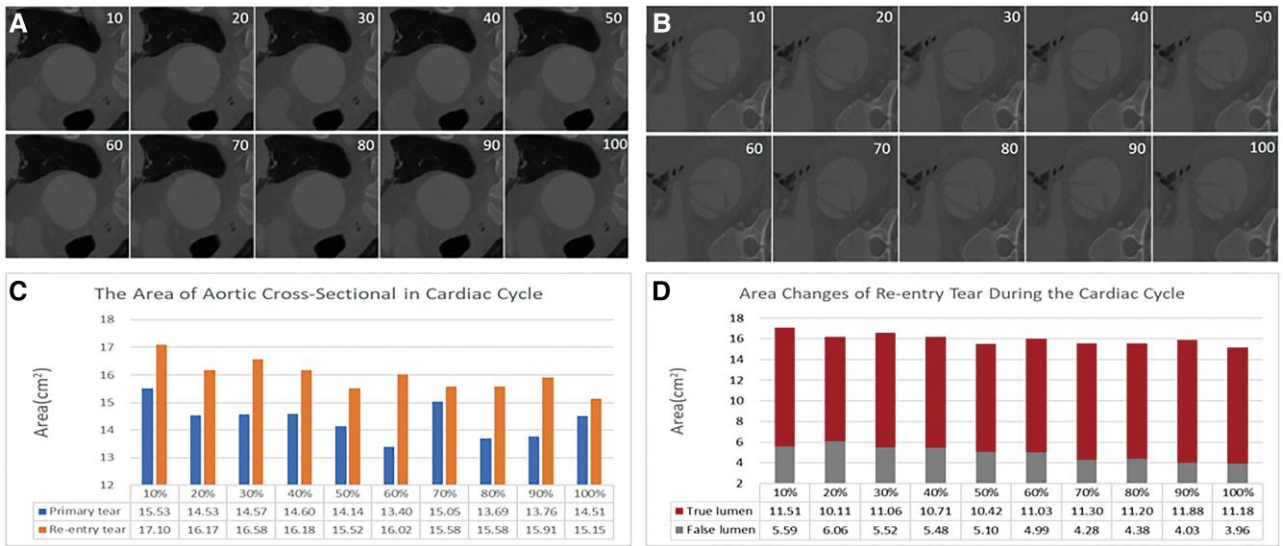
Figure 4 Images and areas of the primary and re-entry tears (true and false lumen) at 10 phases of the cardiac cycle. (A) Cross-sectional image of the primary tear. (B) Cross-sectional image of the re-entry tear. (C) Graph showing that the changes in the area of the re-entry tear are greater than those in the primary tear during the cardiac cycle. (D) Graph showing that the changes in area of the false lumen are greater than those in the area of the true lumen. The intimal flap entering and exiting the opening from the 10 phase cross-sectional images showed that the luminal area at the entrance (A) was smaller than that at the exit (B), and the morphological changes in the intimal flap at the re-entry site were also greater than those at the primary tear site. The luminal areas of the primary tear and re-entry tear in aortic dissection were 14.38 ± 0.65 and 15.98 ± 0.57 cm^2, respectively, and the areas of the true and false lumens at the re-entry site were 11.04 ± 0.52 and 4.94 ± 0.73 cm^2, respectively, as shown by further measurements. Although the area of the re-entry tear was larger than that of the primary tear overall, its fluctuation with blood flow was less than that of the primary tear, and the amplitude of the change in the area of the true lumen was greater than that of the false lumen.
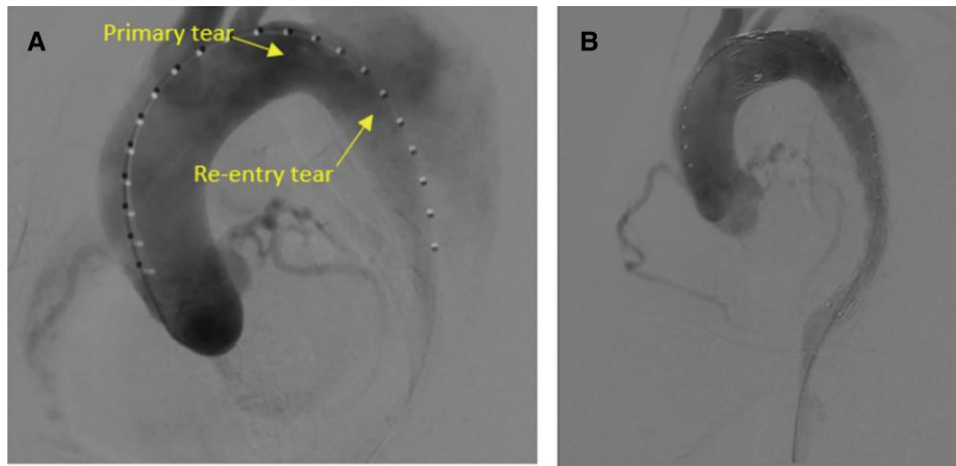

Figure 5 Intraoperative angiography. (A) Digital subtraction angiography video before stent placement showing the re-entry tear from the false lumen to the true lumen. (B) Satisfactory isolation of the main rupture site and false lumen associated with the aortic dissection was revealed.

Correspondingly, the expansion ratio of the true and false lumens at the re-entry site mirrored this, also being 3:1. We utilized the viscoelastic formula $DPa^{-1} = \frac{\Delta A}{A_0 \Delta P}$ [10] to calculate the ratio of viscoelasticity between the true and false lumens (*Figure 4B and D*), reflecting their relative expansions within the cardiac cycle as $D_{radio} = \frac{D_F}{D_T} = 3.019 \approx 3:1$. The distinct dilation behaviours of the true and false cavities were denoted as D_T and D_F, respectively. It is worth mentioning that the expansion ratio

between the true and false lumens was consistent with the diameter ratio between the primary and re-entry tears. This suggests that post-dissection rupture, a dynamic equilibrium within the internal blood flow was established. Such a balance may have been a pivotal factor in the patient's survival post-ruptured aortic dissection. While no definitive conclusion on the mechanism underlying can be discerned from an isolated case report, we wish to prompt future research to

delve deeper into the predictive significance of diverse 4D-CT flow-derived parameters.

In this case of triple-lumen complicated TBAD, 4D-CT was employed for visualization analysis and to assess geometric changes following rupture. The technique demonstrated the potential in analysing complex aortic dissections by enabling the visualization of intimal flap spatial distribution and the assessment of dissection risk within a realistic, intricate blood flow environment. Additionally, 4D-CT offers the benefits of non-invasive and rapid scanning.

The intricate pathological features and haemodynamics of this condition pose considerable challenges for guidewire and catheter navigation in implantation procedures. Surgeons must precisely identify the true lumen, with accurate localization of the dissection entry point being paramount for precise angiography and stent deployment. Measurement of aortic diameter and assessment of dissection extent enable clinicians to predict future patient outcomes. Consequently, the provision of quantitative data and blood flow visualization to clinicians is vital for the formulation of effective treatment strategies and the optimization of patient prognosis.

Lead author biography

Ying Li is an associate professor in the Department of Biomedical Engineering and Imaging Medicine. She is interested in research in the fields of digital medicine and cardiovascular disease, with a focus on the study of aortic and coronary artery diseases, as well as imaging technologies.

Jia Li works as an attending doctor in the Department of Emergency, the Second Affiliated Hospital of Army Medical University, mainly engaged in EICU-related work, and is good at the diagnosis and treatment of diseases in emergency, such as acute poisoning, aortic dissection, multiple organ failure, cardiopulmonary cerebral resuscitation, and other critical diseases.

Acknowledgements

Data availability

In consideration of the privacy of the individual involved in the study, the raw images during the research process will not be made publicly available. However, interested researchers may request access to the data by contacting the corresponding author, adhering to ethical and data policy frameworks.

References

1. Carrel T, Sundt TM III, von Kodolitsch Y, Czerny M. Acute aortic dissection. *Lancet* 2023;**401**:773–788.
2. Costello JE, Cecava ND, Tucker JE, Bau JL. CT radiation dose: current controversies and dose reduction strategies. *AJR Am J Roentgenol* 2013;**201**:1283–1290.
3. MacGillivray TE, Gleason TG, Patel HJ, Aldea GS, Bavaria JE, Beaver TM, et al. The Society of Thoracic Surgeons/American Association for Thoracic Surgery Clinical Practice Guidelines on the management of type B aortic dissection. *Ann Thorac Surg* 2022;**113**:1073–1092.
4. Norton EL, Farrington WJ, Keeling WB, Wei JW, Binongo JN, Zellner AB, et al. Acute-on-chronic aortic dissection: management and outcomes of the unstable "triple-lumen" aorta. *Ann Thorac Surg* 2024;**117**:923–930.
5. Mazzolai L, Teixido-Tura G, Lanzi S, Boc V, Bossone E, Brodmann M, et al. 2024 ESC guidelines for the management of peripheral arterial and aortic diseases. *Eur Heart J* 2024;**45**:3538–3700.
6. Saitta S, Guo B, Pirola S, Menichini C, Guo D, Shan Y, et al. Qualitative and quantitative assessments of blood flow on tears in type B aortic dissection with different morphologies. *Front Bioeng Biotechnol* 2021;**9**:742985.
7. Isselbacher EM, Preventza O, Hamilton Black J III, Augoustides JG, Beck AW, Bolen MA, et al. 2022 ACC/AHA Guideline for the Diagnosis and Management of Aortic Disease: a report of the American Heart Association/American College of Cardiology Joint Committee on Clinical Practice Guidelines. *Circulation* 2022;**146**:e334–e482.
8. Wang Q, Guo X, Stäb D, Poon JN, Lim EKW, Lim RP, et al. Computational fluid dynamic simulations informed by CT and 4D flow MRI for post-surgery aortic dissection—a case study. *Int J Heat Fluid Flow* 2022;**96**:108986.
9. Zimmermann J, Bäumler K, Loecher M, Cork TE, Marsden AL, Ennis DB, et al. Hemodynamic effects of entry and exit tear size in aortic dissection evaluated with in vitro magnetic resonance imaging and fluid–structure interaction simulation. *Sci Rep* 2023;**13**:22557.
10. Ganten MK, Weber TF, von Tengg-Kobligk H, Böckler D, Stiller W, Geisbüsch P, et al. Motion characterisation of aortic wall and intimal flap by ECG-gated CT in patients with chronic B-dissection. *Eur J Radiol* 2009;**72**:146–153.